

Behaviour of a plane joint under horizontal cyclic shear loading

Wengang Dang^{*1,2,3}, Thomas Frühwirt^{3a} and Heinz Konietzky^{3b}

¹State Key Laboratory of Water Resources and Hydropower Engineering Science, Wuhan University,
No. 8 Donghu South Road, Wuhan 430072, China

²State Key Laboratory for GeoMechanics and Deep Underground Engineering,
China University of Mining and Technology, Beijing, China

³Institute of Geotechnics, TU Bergakademie Freiberg, Gustav-Zeuner-Straße 1, 09599 Freiberg, Germany

(Received May 9, 2016, Revised May 15, 2017, Accepted May 16, 2017)

Abstract. This paper describes lab test results of artificial rock-like material samples having a plane joint. Cyclic shear tests were performed under different normal loads and different shear displacement amplitudes. For this purpose, multi-stage normal loading tests (30 kN, 60 kN, 90 kN, 180 kN, 360 kN and 480 kN) with cyclic excitation at frequency of 1.0 Hz and different shear displacement amplitudes (0.5 mm, 1.0 mm, 2.0 mm, 4.0 mm, 5.0 mm, and 8.0 mm) were conducted using the big shear box device GS-1000. Experimental results show, that shear forces increase with the increase of normal forces and quasi-static friction coefficient is larger than dynamic one. With the increase of normal loads, approaching the peak value of shear forces needs larger shear displacements. During each cycle the normal displacements increase and decrease (rotational behavior in every cycle). Peak angle of inclination increases with the increase of normal load. A phase shift between maximum shear displacement and maximum shear force is observed. The corresponding time shift decreases with increasing normal load and increases with increasing shear displacement amplitudes.

Keywords: joint; cyclic loading; shear box device; direct shear test; lab testing

1. Introduction

Stability and service ability of civil and mining engineering projects have to consider the existence and the behavior of joints in the rock mass. The presence of discontinuities often reduces the strength and stiffness of the rock. Understanding the shear behaviour of jointed rock masses is very important for many engineering projects (e.g., for surface and underground excavations, dam foundations or geothermal reservoirs) and for avoiding geological hazards (Hoek and Brown 1980, Hoek and Bray 1981, Babanouri *et al.* 2011, Liu *et al.* 2012, 2013, Liu and Dang 2014, Li *et al.* 2016a, b). In order to get a deeper understanding of the shear behaviour of joints, direct shear box tests under constant normal load (CNL) and constant normal stiffness (CNS) conditions are becoming increasingly popular, and got attention by several researchers in the recent past (e.g.,

*Corresponding author, Ph.D., E-mail: dbzkd@126.com

^aPh.D., E-mail: thomas.fruehwirt@ifgt.tu-freiberg.de

^bPh.D., E-mail: heinz.konietzky@ifgt.tu-freiberg.de

Barton and Choubey 1977, Lee *et al.* 2014, Nguyen *et al.* 2013, 2014, Dang *et al.* 2016a, 2017, Dang 2017). Due to blasting or earthquake excitation, rock masses suffer dynamic loadings. Therefore, dynamic effects on rock masses need to be considered and several researchers investigated the rock behaviour under dynamic loading conditions (e.g., Crawford and Curran, 1981, Kana *et al.* 1996, Lee *et al.* 2001, Jafari *et al.* 2003, Bagde and Petros 2005, Belem *et al.* 2007, Guo *et al.* 2011, Liu *et al.* 2011, 2012, Konietzky *et al.* 2012, Cabalar *et al.* 2013, Nguyen *et al.* 2014, Tao *et al.* 2012, 2013a, 2013b, 2015, Xu *et al.* 2015, Zhou *et al.* 2015, 2017, Dang *et al.* 2016b, Dang 2017, Li *et al.* 2017).

Bagde and Petros (2005) studied the fatigue properties of intact sandstone under different waveforms, amplitudes and frequencies. They concluded that all these three factors have great effect on the fatigue properties. The most critical damage was observed applying square waves with low frequency and low amplitude. Guo *et al.* (2011) investigated the fatigue damage and irreversible deformation of salt rock under uniaxial cyclic loading. They found that fatigue life of rocks is mainly influenced by its structure as well as applied stress amplitude. Liu *et al.* (2011, 2012) carried out axial cyclic loading tests on sandstone samples. They recognized that under large confining pressure the samples failed after fewer cycles. They also found, that axial strain and number of cycles up to failure increase with increasing frequency. Lee *et al.* (2001) investigated the asperity degradation of rough rock joints under cyclic shear loading. Cyclic shear lab tests were conducted for two joint types of Hwangdeung granite and Yeosan marble: Saw-cut and split tensile joints. They found high peak shear strength and non-linear dilation in the first loading cycle, different frictional resistance for the reverse shear loading direction, anisotropic shear behavior and its dependence on the normal stress level. Jafari *et al.* (2003) studied the variation of the shear strength of rock joints under cyclic loading and found, that shear strength of joints is related to shear velocity, number of loading cycles and stress amplitudes. Belem *et al.* (2007) conducted cyclic shear tests of specimens with different shapes and proposed two rock joint surface roughness degradation models to predict the variation of joint surface degradation during monotonic and cyclic shearing. Ferrero *et al.* (2010) performed cyclic shear tests with frequencies ranging from 0.013 to 3.9 Hz and maximum displacements between 1.0 and 4.0 mm. They found that shear strength decrease is strongly dependent on amplitudes. Konietzky *et al.* (2012) have developed a new large dynamic direct shear box device called GS-1000 for both quasi-static and dynamic tests. Dynamic tests were conducted on shale stone samples with dynamic normal load (earthquake signal) of about 550 kN and a shear load of about 300 kN. They found that shear strength decreases with ongoing shear displacement and the dynamic input also leads to a further settlement (joint closure) of the sample. Thevenet *et al.* (2013) investigated the behavior of adhesively bonded joints under cyclic shear loading with different impact amplitudes. They underlined, that the evolution of viscous deformations and damage depends on the loading type. Mirzaghobanali *et al.* (2014) performed cyclic shear tests in the lab on artificial rock joints with different shear rates and initial normal stresses under CNS conditions and found that shear strength decreases with increase in the loading cycles and shear rate. When the normal force was increased, the effect of shear rate became less pronounced. Nguyen *et al.* (2014) conducted cyclic shear tests on Mayen-Koblenz slate and found, that peak shear stress of the jointed rock under dynamic loading shows tendency to increase with time. Depending on the joint orientation the peak shear stresses are higher or lower in the positive or negative shear direction, respectively. The peak shear stress under dynamic loading is approximately 30% higher than that under static loading. The normal stress was nearly constant during cyclic shearing. Dang *et al.* (2016a, b) performed static and dynamic shear tests on planar joints. They found that shear forces and sample inclination

(rotation) of the specimen increase with increasing normal load and decrease with increasing shear speed under quasi-static conditions, and force distribution at the joint becomes very inhomogeneous during shearing. Under dynamic normal load conditions, shear force and friction coefficient show cyclic behaviour, characterized by significant time shift between normal and shear force (shear force delay), between normal force and friction coefficient (friction coefficient delay). Also, the relative time shift between peak normal force and peak shear force decreases with increasing impact amplitudes; the relative time shift between peak normal force and peak friction coefficient is nearly constant. Finally, they proposed a new shear strength criterion for joints under constant shear velocity and sinusoidal normal loading.

ISRM suggested methods for lab shear tests recommend the use of three to four transducers to measure vertical displacement (Muralha *et al.* 2014). However, due to the limitations of the shear box devices, in former studies scientists were always taking the average normal displacements of the jointed specimen to evaluate the dilation during cyclic shearing (Kana *et al.* 1996, Nguyen *et al.* 2014). However, detailed consideration shows that normal displacements of the top specimen at different observation points are significantly different (Dang *et al.* 2016a, b, 2017). Considering only average normal displacements leads to a loss of information and prevents a deeper understanding of joint behavior under cyclic shearing.

The aim of this study is to investigate the cyclic shear behaviour of artificial jointed specimens having a smooth plane joint surface. Special attention was paid to the influence of normal loads and shear displacement amplitudes. Normal loads varied from 30 kN to 480 kN, shear displacement amplitudes varied from 0.5 mm to 8.0 mm. Normal displacements of the top specimen were measured at the four corners by four Linear Variable Differential Transformers (LVDTs) with high accuracy (± 0.001 mm).

2. Laboratory investigation

2.1 GS-1000 shear box device

The cyclic shear tests were performed using the GS-1000 shear box device (Fig. 1). GS-1000 shear box device was developed in 2012 at the Chair of Rock Mechanics at the TU Bergakademie Freiberg, Germany (Konietzky *et al.* 2012). Hydraulic aggregate, shear box with horizontal and vertical frame, electronic control unit and water cooling system are the most important components. The main technical specifications of the GS-1000 apparatus are given in Table 1. As shown in Fig. 1(c), shear displacement is measured by a horizontal LVDT, which is attached to the bottom part of the shear box. The normal displacement is measured by four vertical LVDTs, which were positioned at the four corners of the upper part of the shear box. Normal and shear loads were measured by load-cells integrated in the vertical and horizontal loading pistons.

Table 1 Main technical data of GS-1000 shear box device

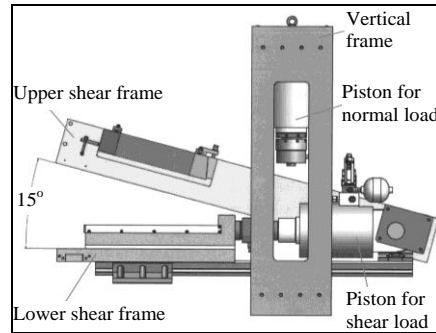
Item	Value
Normal force	from 0 kN to +1000 kN
Shear force	from -300 kN up to +800 kN
Maximum shear displacement	50 mm
Shear velocity	from $<1e-7$ mm/s up to 70 mm/s

Table 1 Continued

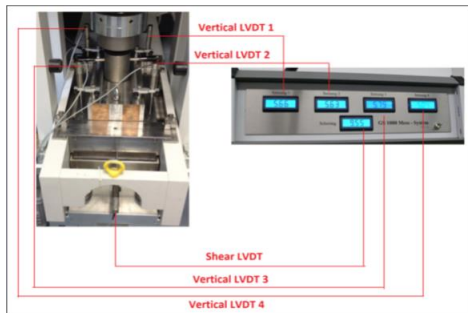
Item	Value
Frequency	from 0 Hz to 40Hz
Dynamic loading	-500 kN up to +500 kN superimposed on static force level



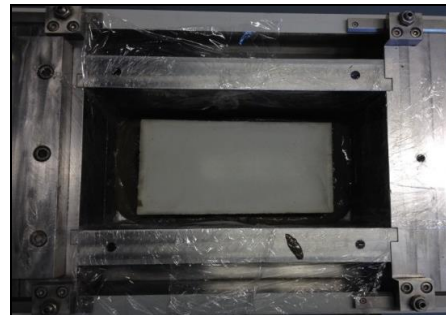
(a) Test apparatus



(b) Main components



(c) LVDTs and data logging unit AM8

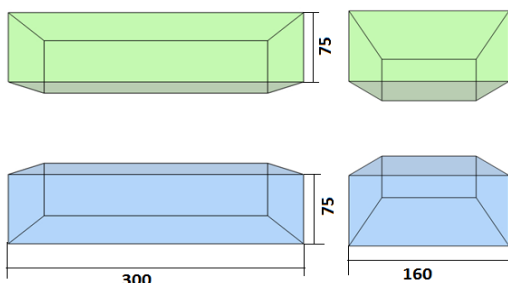


(d) Shear box with the specimen inside

Fig. 1 GS-1000 shear box device (Konietzky *et al.* 2012)

Table 2 Mechanical parameters of concrete specimen

Item	Tensile strength (MPa)	Uniaxial compressive Strength (MPa)	Young's modulus (GPa)	Poisson ratio	Cohesion (MPa)	Internal friction angle (°)	Dilation angle (°)	Density (g/cm ³)
Concrete	2.5	19.1	30	0.2	7.2	30	10	2.50



(a) Geometry and size (unit: mm)



(b) Real sample

Fig. 2 Lab samples

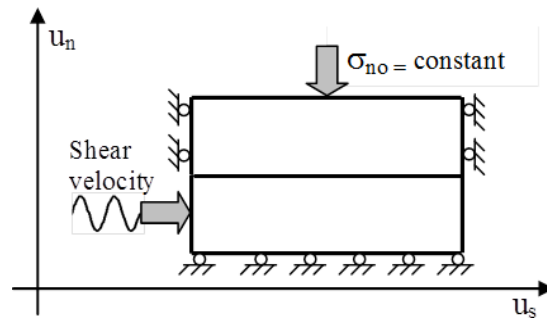


Fig. 3 Set-up of cyclic shear test (CNL-test)

Table 3 Test schemes

Sample	Stage	F_n	f	u_s
		(kN)	(Hz)	(mm)
DT_0	1	30	0	20
	2	60	0	20
	3	90	0	20
	4	180	0	20
	5	240	0	20
	6	360	0	20
DT_1	1	30	1	5
	2	60	1	5
	3	90	1	5
	4	180	1	5
	5	240	1	5
	6	360	1	5
	7	480	1	5
DT_2	1	30	1	0.5
	2	30	1	1
	3	30	1	2
	4	30	1	4
	5	30	1	8
DT_3	1	90	1	0.5
	2	90	1	1
	3	90	1	2
	4	90	1	4
	5	90	1	8
DT_4	1	180	1	0.5
	2	180	1	1
	3	180	1	2
	4	180	1	4
	5	180	1	8

2.2 Laboratory test set-up

To have several samples with nearly identical properties available, concrete replicas of jointed rocks were used in this study. The replicas were made from the same concrete and have nearly identical matrix and surface properties, which allows to perform several shear experiments with nearly identical samples and consequently, to study the influence of different loading parameters on the shear behaviour. The size of the specimen was 300 mm×160 mm×150 mm (length/width/height) (Fig. 2). The specimens were made of CEM I 32.5 R cement and Hohenpockaer glasssand with weight ratio of 1:3. The mechanical properties of the material tested after 28 days are shown in Table 2.

In this research, the cyclic loading was applied as a dynamic excitation in the horizontal direction applying an additional constant normal load on top of the specimen (Fig. 3).

The shear displacement controlled sinusoidal excitation was applied horizontally to the bottom part of specimen as follows

$$u_s = u_{\max} \sin(2\pi ft) \quad (1)$$

u_s ... Shear displacement

u_{\max} ... Amplitude of shear displacement

f ... Frequency

t ... Time

All cyclic tests (10 shearing-cycles at each normal load level) were performed with a frequency of 1.0 Hz (as preliminary investigations have shown, in the range between 0.25 to 2.0 Hz shear frequency has little influence on the peak shear force and dilation, therefore, only tests with 1.0 Hz are presented within this paper). For comparison also simple static shear tests (DT_0) were performed. For sample DT_1, the shear amplitude was maintained close to ± 5.0 mm. The constant normal loads applied on top of the specimen were 30 kN, 60 kN, 90 kN, 180 kN, 360 kN and 480 kN, respectively. For samples DT_2, DT_3, DT_4, keeping the frequency at 1.0 Hz, the shear displacement amplitude was maintained close to ± 0.5 mm, ± 1.0 mm, ± 2.0 mm, ± 4.0 mm and ± 8.0 mm, respectively, and the constant normal loads applied on top of the specimen were 30 kN, 90 kN and 180 kN, respectively. The specific test schemes are shown in Table 3.

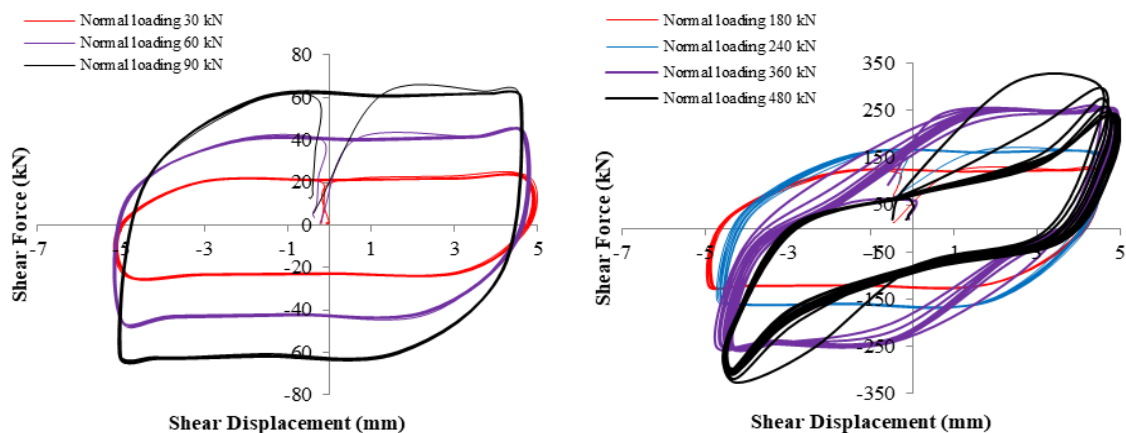


Fig. 4 Shear force versus time for different normal loads (shear displacement amplitude 5.0 mm)

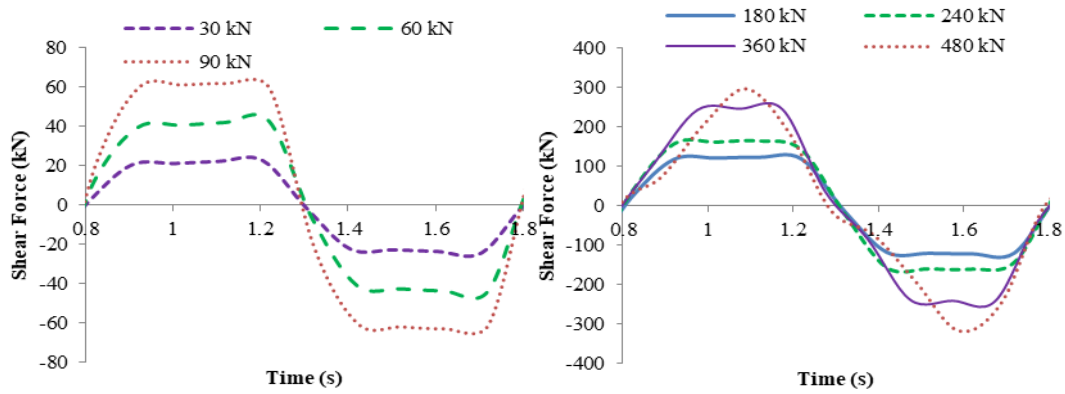
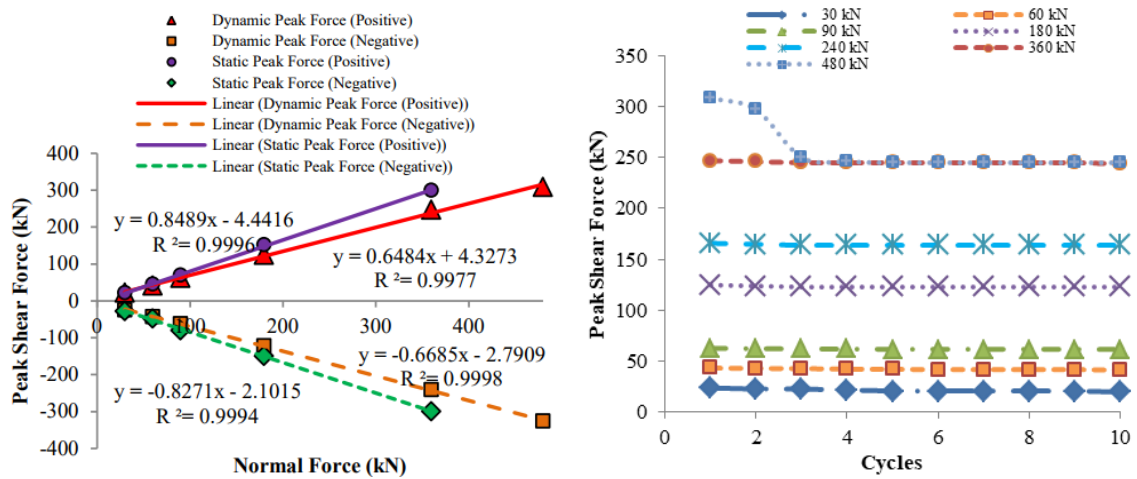


Fig. 5 Shear force versus time under different normal loads (shear displacement amplitude 5.0 mm)



(a) Peak shear forces in push and pull directions (b) Peak shear forces within cycles in push direction

Fig. 6 Peak shear force changing behaviour

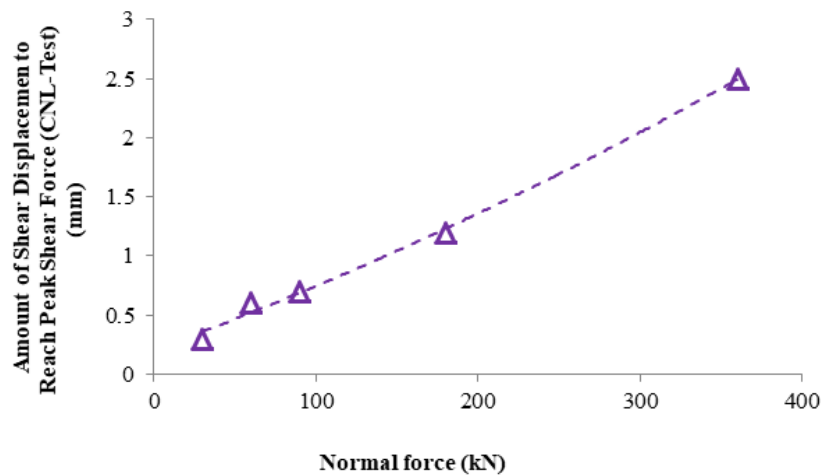


Fig. 7 Amount of shear displacement to reach peak shear force under different normal loads

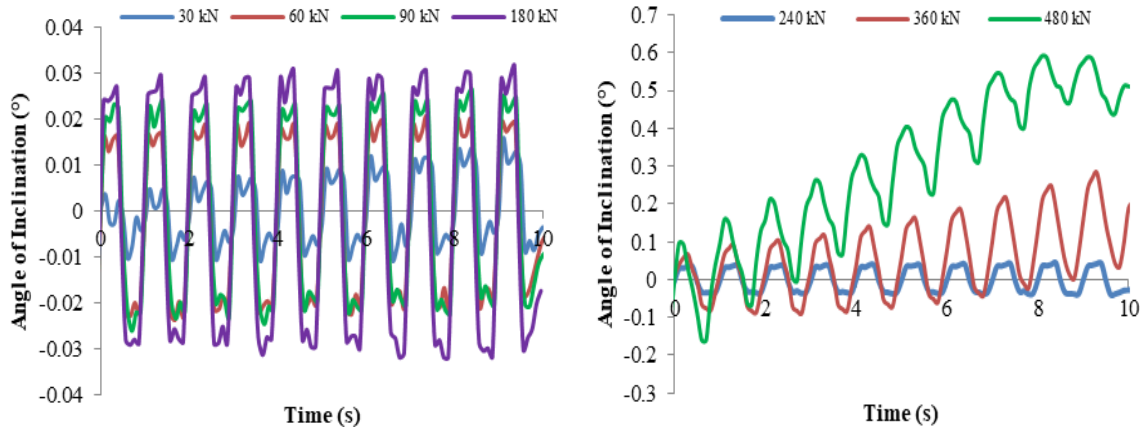
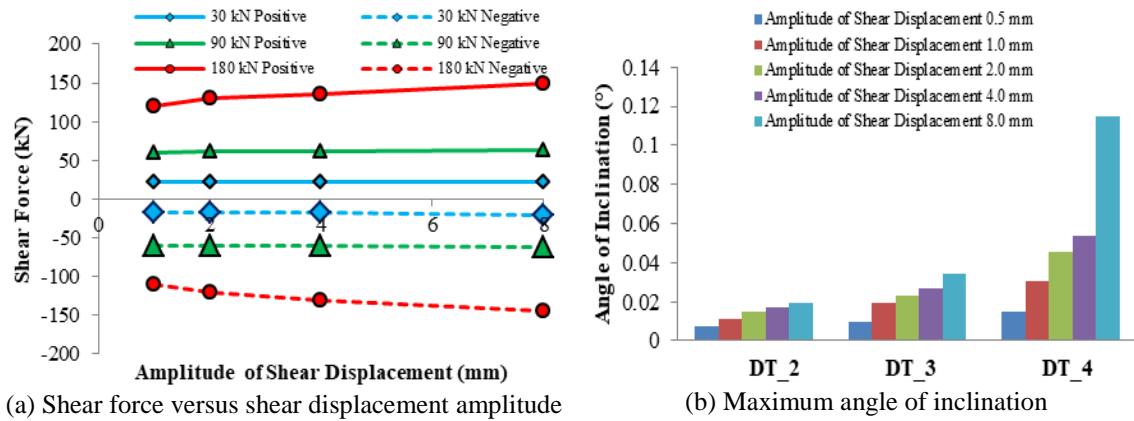


Fig. 8 Angle of inclination versus time under different normal loads



(a) Shear force versus shear displacement amplitude

(b) Maximum angle of inclination

Fig. 9 Cyclic shear behaviour influenced by shear displacement magnitudes

3. Tests results

3.1 Tests under different normal loads, but same shear displacement amplitudes

Figs. 4-6 show that peak shear forces increase with increasing normal loads. The absolute values of peak shear force in the positive shear direction (push direction) and in the negative shear direction (pull direction) are more or less the same. Under low normal loads (loads below 240 kN), shear forces increase with shear displacement dramatically and the peak value is reached after short shear displacement and keeps constant. With the increase of normal loads, larger shear displacements are necessary to reach the peak shear force (also demonstrating in Fig. 7, larger normal force needs longer shear displacement to peak shear force). Under higher normal loads (loads above 360 kN), the shape of the curve of shear forces versus shear displacements changes. After several cycles, under a normal load of 480 kN and up to shear displacements of about ± 2.0 mm, the induced shear forces are below 100 kN. This is smaller than under the normal force of 180 kN, 240 kN or 360 kN. Consequently, the general conclusion that shear forces increase with increasing normal loads is no longer true. This statement is valid only for low normal loads (in our

case below 240 kN). As indicated by the results documented in Fig. 5 contact surface is damaged seriously under high normal loads and the friction coefficient of the interface becomes smaller in a certain area. After extended shear displacement, induced shear forces increase and reach the peak value. Peak shear forces reduce with the increase of cyclic shear cycles and finally reach a constant value (Fig. 6(b)).

When considering only the peak state, the relationship between the maximum values of shear forces in push and pull direction, respectively, and normal forces are nearly linear (Fig. 6(a)). Compared with the peak values of shear forces under static conditions, the peak shear forces registered during cyclic tests show lower values, in other words, the friction angle is somewhat smaller in a cyclic shearing progress.

We calculated the rotation of the upper part of the specimen using the formula

$$\alpha = \arctan\left(\frac{|u_{n(a)}| + |u_{n(b)}|}{l_{\text{Specimen}}}\right) \quad (2)$$

$u_{n(a)}$... Normal displacement of left side

$u_{n(b)}$... Normal displacement of right side

l_{Specimen} ... Total length of specimen (=300 mm)

Fig. 8 shows the vertical movement of the top specimen during cyclic shearing. Rotation occurs during each cycle. Under low normal load (below 240 kN), normal displacements reduce on one side and increase on the other side of the sample. The corresponding angle of inclination is increasing until a peak value is reached. During this period, the top specimen shows an anticlockwise rotational trend and finally reaches a plateau level. Afterwards, the normal displacements increase at the left side and reduce at the right side and the corresponding angle of inclination is decreasing. Finally, a peak state with plateau is reached again and movement starts in the opposite direction. During this period, the top specimen shows a clockwise rotation until the peak state is reached. At 30 kN normal force, the maximum angle of inclination is 0.001 degree, while it reaches 0.003 degree under a normal force of 180 kN. It is indicated that rotation increases with increasing normal loads. However, when normal load exceeds 360 kN, the inclination towards the positive side (push direction) is increasing during each cycle. This implies that settlement of the top specimen increases step by step and the purely rotational behaviour is superimposed with a major translational component. This is mainly caused by wear of the joint surfaces followed by damage of the specimen and is in agreement with curves shown in Fig. 4.

The tests results shown above indicate that in order to avoid damage of the specimen during the cyclic loading, normal loads should be kept below 240 kN. Therefore, only normal loads of 30 kN, 90 kN and 180 kN were chosen to investigate the cyclic shear behaviour influenced by different shear displacement amplitudes.

3.2 Tests under different shear displacement amplitudes

Fig. 9 illustrates how the cyclic shear behaviour is influenced by shear displacement magnitudes. Fig. 9(a) indicates that shear forces increase with increasing normal loads. Under the same normal load, peak shear forces are nearly independent on the shear displacement amplitude. This is in contrast to joints having asperities. Fig. 9(b) shows the rotation under different shear displacement amplitudes and different normal loads. Considering the same shear displacement amplitudes, higher normal loads give a bigger angle of inclination. This is in agreement with results shown in Fig. 8. Under same normal load, the rotation increases with increasing shear

displacements.

4. Discussion

4.1 Movement behaviour

The undesired rotation is caused by a force redistribution which leads to moments and consequently inclination (rotation) of the sample. This phenomenon was simulated with the help of a numerical model. The whole model consists of several parts: loading plate, lower shear box, upper shear box, lower and upper part of specimen and corresponding interfaces. Size and shape as well as initial and boundary conditions are identical to that of the lab tests. The numerical model consists of 34403 grid points, 27600 zones, 3417 interface nodes and 6312 interface elements. Normal force is applied at the loading plate. The top shear box is fixed in vertical and horizontal direction. The cyclic shear velocity is applied to the lower shear box. A Mohr-Coulomb constitutive model is chosen for the specimen and interfaces and an elastic constitutive model is chosen for the shear box. Mechanical parameters are shown in Table 2. As illustrated in Fig. 10 the reaction forces and principal stresses are uniformly distributed after applying the normal load. However, with ongoing shear displacement reaction forces become more and more non-uniform. Consequently, movements develop, which lead to sample rotation, which is explained in more detailed by Dang *et al.* (2016a, 2017). Also, it is evident that the area in contact is decreasing during the shearing progressed and therefore, stresses at the joint increase. This has to be considered in the test data evaluation.

Nguyen *et al.* (2014) reported that during the cyclic shear tests shear movement of one cycle can be subdivided into four phases: Forward advance, forward return, backward advance and backward return. They only considered the average normal displacement at midpoint of the specimen top to evaluate the vertical movement of the top specimen. We instead consider in detail the rotational component. The normal displacements at the two ends of the specimen are different, and the frequency of average normal displacement measured at the top of the specimen is twice the input frequency. Shear and normal displacements versus time under normal load of 90 kN, shear displacement frequency of 1.0 Hz and shear amplitude of 5.0 mm are shown in Fig. 11 for two cycles.

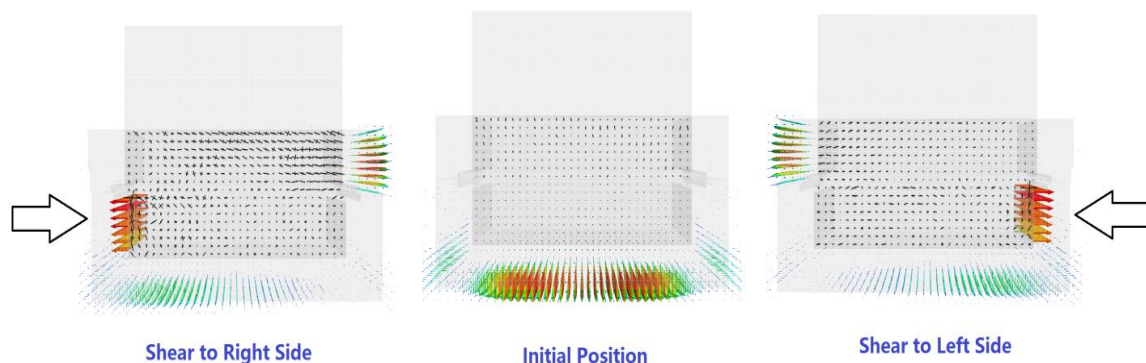


Fig. 10 Reaction forces and principal stresses distribution at different shear stage

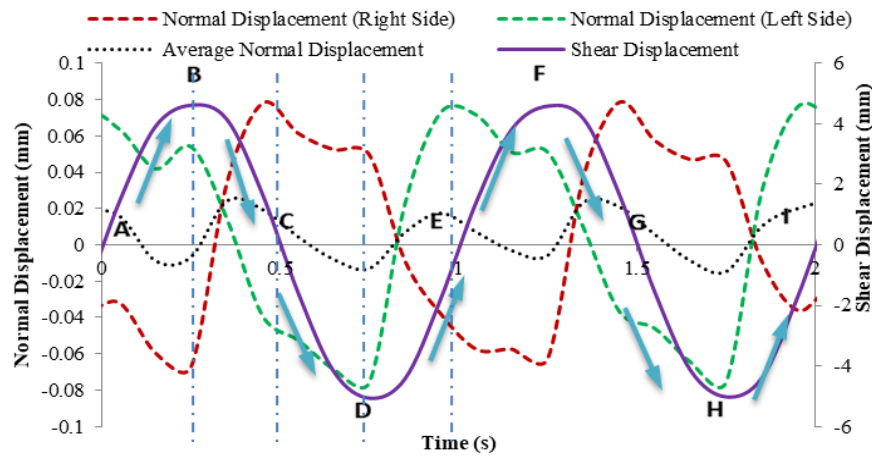


Fig. 11 Shear and normal displacement versus time (frequency 1.0 Hz, normal load 90 kN). Negative values for normal displacement indicate dilational behaviour. Positive values for shear displacement indicate push-direction

The four phases inside one cycle can be characterized as follows:

Phase I (A to B): Forward advance. The bottom specimen moves in the forward (push) direction. After initial uniform dilation the left side of the top specimen shows compaction while the right side continuously shows dilational behaviour. The amplitude of heave and settlement increases with increasing shear displacement. The top part of the specimen experiences uplift.

Phase II (B to C): Forward return. The bottom specimen is moving into the opposite direction. The left side of the top specimen moves upwards and the right side moves downwards. The amplitude of heave and settlement decreases with increasing shear displacement. The average vertical movement is positive (downward direction, joint closure). At point C, the sample has reached again the initial position.

Phase III (C to D): Backward advance. Bottom specimen is still moving into the opposite direction. At the left side, upward movement is still observed and at the right side movement direction is changed from compaction to dilation. The amplitude of heave increases with increasing shear displacement. The average vertical movement is negative indicating dilation.

Phase IV (D to E): Backward return. The movement direction of the bottom specimen reverses and has the same direction as in phase I. Normal displacement decreases at the left side and increases at the right side. The amplitude of heave and settlement increases with increasing shear displacement. The specimen shows compactional behavior in that phase.

4.2 Time shift

Fig. 12 shows the relationship between measured shear force and shear displacement versus time for two different normal loads. This figure reveals a phase shift between the points of reaching maximum shear displacement and maximum shear force. The shear displacement is phase lagging with shear force. This behaviour is observed during all experiments. Our results are similar to those reported by Ahola *et al.* (1996) and Nguyen *et al.* (2014). Ahola *et al.* (1996) explained the phase shift with chatter of the joint surface and vibrations of the apparatus. In order to

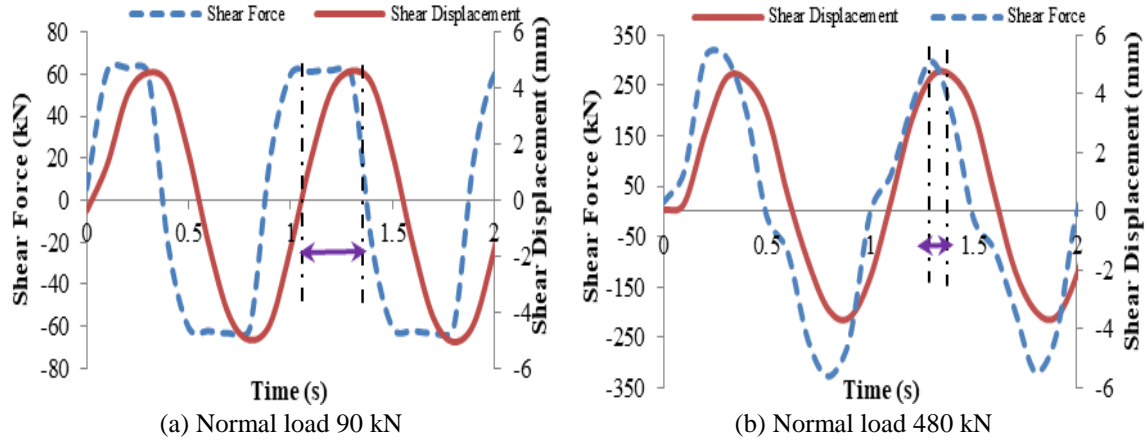


Fig. 12 Shear displacement and shear force versus time

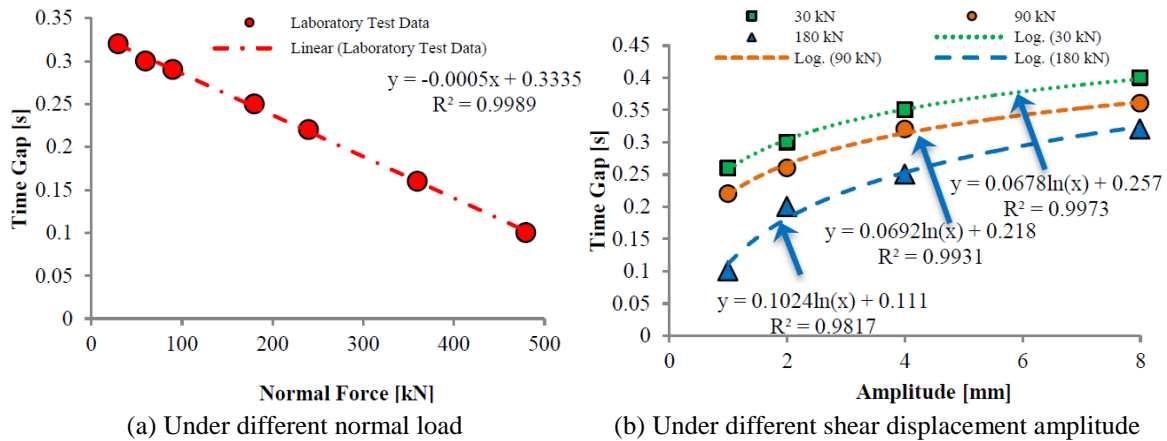


Fig. 13 Time gap

investigate the phase shift during the cyclic shearing in more detail, the influencing factors of normal forces and shear displacement amplitudes were considered.

As documented in Fig. 13(a) for the same shear displacement frequency (1.0 Hz) and same shear displacement amplitude (5.0 mm) a phase shift of 0.225 sec is observed for normal load of 30 kN, whereas a phase shift of only 0.05 sec is observed for normal load of 480 kN. This indicates that phase shift decreases with increasing normal loads. In other words: Under higher normal loads larger shear displacements are necessary to reach the maximum shear force (see Figs. 4 and 7). A corresponding fitting equation can be deduced for the relation between normal load and time gap

$$y = -0.0005x + 0.3335 \quad (R^2 = 0.9989) \quad (3)$$

y...Time gap
 x...Normal load

Fig. 13(b) presents results for evolution of the time gap between max. shear displacement and max. shear force for different normal loads and different shear displacement amplitudes. At a

frequency of 1.0 Hz, normal loads of 30 kN, 90 kN and 180 kN, respectively, and shear displacement amplitude of 1.0 mm, phase shift is 0.26 sec (30 kN), 0.21 sec (90 kN) and 0.1 sec (180 kN), respectively. However, it is 0.41 sec (30 kN), 0.33 sec (90 kN) and 0.27 sec (180 kN) considering a shear displacement amplitude of 8.0 mm. This indicates that phase shift increases with increasing shear displacement amplitude. Fitted equations for the relation between shear displacement amplitude and time gap are deduced as follows

$$y=0.0678\ln(x)+0.257 \quad (R^2=0.9973) \text{ for normal load of 30 kN} \quad (4)$$

$$y = 0.0692\ln(x) + 0.218 \quad (R^2 = 0.9931) \text{ for normal load of 90 kN} \quad (5)$$

$$y = 0.1024\ln(x) + 0.111 \quad (R^2 = 0.9817) \text{ for normal load of 180 kN} \quad (6)$$

y...Time gap

x...Shear displacement amplitude

It can be concluded, that phase shift between shear forces and shear displacements is influenced by both, normal load and shear displacement amplitude.

5. Conclusions

This paper discusses a study of the variation in shear strength of a plane joint replica in different cyclic loading conditions. The following main conclusions may be drawn from this investigation.

- Peak shear forces increase with increasing normal loads and friction angle is smaller in a cyclic shearing progress than in a quasi-static shearing test.
- During each cycle the normal displacements increase and decrease (rotational behavior in every cycle), peak angle of inclination increases with increasing of normal force and shear displacement amplitude. And, the unwanted rotation is caused by uneven force distribution during shearing.
- Peak shear forces are nearly independent on the shear displacement amplitudes.
- There is a phase shift between maximum shear displacement and maximum shear force. The corresponding time gap decreases with increasing normal load and increases with increasing shear displacement amplitude.

Acknowledgments

This work was supported by the National Basic Research Program of China (2015CB060200), the National Natural Science Foundation of China (51274254, 51322403, 11402311), the State Key Laboratory for GeoMechanics and Deep Underground Engineering, China University of Mining and Technology (SKLGDUEK1719), and the Open Foundation of State Key Laboratory of Hydrology-Water Resources and Hydraulic Engineering. The first author would like to thank the Chinese Scholarship Council for its financial support provided for his Ph. D study at TU Bergakademie Freiberg, Germany. Special thanks to Mr. Tom Weichmann, Mrs. Beatrice Tauch and Mr. Gerd Mu"nzberger for help during laboratory testing.

References

- Ahola, M.P., Hsiung, S.M. and Kana, D.D. (1996), "Experimental study on dynamic behavior of rock joints", *Dev. Geotech. Eng.*, **79**, 467-494.
- Babanouri, N., Nasab, S.K., Baghbanan, A. and Mohamadi, H.R. (2011), "Over-consolidation effect on shear behavior of rock joints", *J. Rock Mech. Min. Sci.*, **48**(8), 1283-1291.
- Bagde, M.N. and Petros, V. (2005), "Waveform effect on fatigue properties of intact sandstone in uniaxial cyclical loading", *Rock Mech. Rock Eng.*, **38**(3), 169-196.
- Barton, N. and Choubey, V. (1977), "The shear strength of rock joints in theory and practice", *Rock Mech. Rock Eng.*, **10**(1), 1-54.
- Belem, T., Souley, M. and Homand, F. (2007), "Modeling surface roughness degradation of rock joint wall during monotonic and cyclic shearing", *ActaGeotech.*, **2**(4), 227-248.
- Cabalar, A.F., Dulundu, K. and Tuncay, K. (2013), "Strength of various sands in triaxial and cyclic direct shear tests", *Eng. Geol.*, **156**, 92-102.
- Crawford, A.M. and Curran, J.H. (1981), "The influence of shear velocity on the frictional resistance of rock discontinuities", *J. Rock Mech. Min. Sci.*, **18**(6), 505-515.
- Dang, W. (2017), "Shear behaviour of plane joints under CNL and DNL conditions: Lab testing and numerical simulation", Ph.D. Dissertation, Freiberg University of Mining and Technology, Freiberg, Germany.
- Dang, W., Konietzky, H. and Frühwirth, T. (2016a), "Rotation and stress changes of a plane joint during direct shear tests", *J. Rock Mech. Min. Sci.*, **89**, 129-135.
- Dang, W., Konietzky, H. and Frühwirth, T. (2016b), "Shear behaviour of a plane joint under dynamic normal load (DNL) conditions", *Eng. Geol.*, **213**, 133-141.
- Dang, W., Konietzky, H., Herbst, M. and Frühwirth, T. (2017), "Complex analysis of shear box tests with explicit consideration of interaction between test device and sample", *Measure.*, **102**, 1-9.
- Ferrero, A.M., Migliazza, M. and Tebaldi, G. (2010), "Development of a new experimental apparatus for the study of the mechanical behaviour of a rock discontinuity under monotonic and cyclic loads", *Rock Mech. Rock Eng.*, **43**(6), 685-695.
- Guo, Y.T., Zhao, K.L., Sun, G.H., Yang, C.H., Ma, H.L. and Zhang, G.M. (2011), "Experimental study of fatigue deformation and damage characteristics of salt rock under cyclic loading", *Rock Soil Mech.*, **32**(5), 1353-1359.
- Hoek, E. and Bray, J.D. (1981), *Rock Slope Engineering*, Taylor & Francis, London, U.K.
- Hoek, E. and Brown, E.T. (1980), *Underground Excavations in Rock*, The Institution of Mining and Metallurgy, London, U.K.
- Jafari, M.K., Hosseini, K.A., Pellet, F., Boulon, M. and Buzzi, O. (2003), "Evaluation of shear strength of rock joints subjected to cyclic loading", *Soil Dyn. Earthq. Eng.*, **23**(7), 619-630.
- Kana, D.D., Fox, D.J. and Hsiung, S.M. (1996), "Interlock/friction model for dynamic shear response in natural jointed rock", *J. Rock Mech. Min. Sci.*, **33**(4), 371-386.
- Konietzky, H., Frühwirth, T. and Luge, H. (2012), "A new large dynamic rock mechanical direct shear box device", *Rock Mech. Rock Eng.*, **45**(3), 427-432.
- Lee, H.S., Park, Y.J., Cho, T.F. and You, K.H. (2001), "Influence of asperity degradation on the mechanical behavior of rough rock joints under cyclic shear loading", *J. Rock Mech. Min. Sci.*, **38**(7), 967-980.
- Lee, Y.K., Park, J.W. and Song, J.J. (2014), "Model for the shear behavior of rock joints under CNL and CNS conditions", *J. Rock Mech. Min. Sci.*, **70**, 252-263.
- Li, X., Cao, W., Tao, M., Zhou, Z. and Chen, Z. (2016a), "Influence of unloading disturbance on adjacent tunnels", *J. Rock Mech. Min. Sci.*, **84**, 10-24.
- Li, X., Zhou, T. and Li, D. (2016b), "Dynamic strength and fracturing behavior of single-flawed prismatic marble specimens under impact loading with a split-hopkinson pressure bar", *Rock Mech. Rock Eng.*, **50**(1), 29-44.
- Li, X., Tao, M., Wu, C., Du, K. and Wu, Q. (2017), "Spalling strength of rock under different static pre-

- confining pressures”, *J. Imp. Eng.*, **99**, 69-74.
- Liu, E.L., He, S.M., Xue, X.H. and Xu, J. (2011), “Dynamic properties of intact rock samples subjected to cyclic loading under confining pressure conditions”, *Rock Mech. Rock Eng.*, **44**(5), 629-634.
- Liu, E.L., Huang, R.Q. and He, S. (2012), “Effects of frequency on the dynamic properties of intact rock samples subjected to cyclic loading under confining pressure conditions”, *Rock Mech. Rock Eng.*, **45**(1), 89-102.
- Liu, Z.X. and Dang, W.G. (2014), “Rock quality classification and stability evaluation of undersea deposit based on MIRMIR”, *Tunn. Undergr. Sp. Tech.*, **40**(2), 95-101.
- Liu, Z.X., Dang, W.G., He, X.Q. and Li, D.Y. (2013), “Cancelling ore pillars in large-scale coastal gold deposit: A case study in Sanshandao gold mine, China”, *Trans. Nonferr. Met. Soc. Chin.*, **23**(10), 3046-3056.
- Liu, Z.X., Dang, W.G. and He, X.Q. (2012), “Undersea safety mining of the large gold deposit in Xinli District of Sanshandao gold mine”, *J. Miner. Metall. Mater.*, **19**(7), 574-583.
- Mirzaghobanali, A., Nemcik, J. and Aziz, N. (2014), “Effects of shear rate on cyclic loading shear behaviour of rock joints under constant normal stiffness conditions”, *Rock Mech. Rock Eng.*, **47**(5), 1931-1938.
- Muralha, J., Grasselli, G. and Tatone, B. (2014), “ISRM suggested method for laboratory determination of the shear strength of rock joints: Revised version”, *Rock Mech. Rock Eng.*, **47**(1), 291-302.
- Nguyen, V.H. (2013), “Static and dynamic behaviour of joints in schistose rock: Lab testing and numerical simulation”, Ph.D. Dissertation, Freiberg University of Mining and Technology, Freiberg, Germany.
- Nguyen, V.H., Konietzky, H. and Frühwirt, T. (2014), “New methodology to characterize shear behavior of joints by combination of direct shear box testing and numerical simulations”, *Geotech. Geol. Eng.*, **32**(4), 829-46.
- Petros, V. and Bagde, M.N. (2005), “Fatigue properties of intact sandstone samples subjected to dynamic uniaxial cyclical loading”, *J. Rock Mech. Min. Sci.*, **42**(2), 237-250.
- Tao, M., Li, X. and Wu, C. (2012), “Characteristics of the unloading process of rocks under high initial stress”, *Comput. Geotech.*, **45**, 83-92.
- Tao, M., Li, X. and Li, D. (2013a), “Rock failure induced by dynamic unloading under 3D stress state”, *Theor. Appl. Fract. Mech.*, **65**(3), 47-54.
- Tao, M., Li, X. and Wu, C. (2013b), “3D numerical model for dynamic loading-induced multiple fracture zones around underground cavity faces”, *Comput. Geotech.*, **54**(10), 33-45.
- Tao, M. and Li, X. (2015), “The influence of initial stress on wave propagation and dynamic elastic coefficients”, *Geomech. Eng.*, **8**(3), 377-390.
- Thevenet, D., Créachdec, R., Sohier, L. and Cognard, J.Y. (2013), “Experimental analysis of the behavior of adhesively bonded joints under tensile/compression-shear cyclic loadings”, *J. Adhes. Adhes.*, **44**, 15-25.
- Xu, W.J., Li, C.Q. and Zhang, H.Y. (2015), “DEM analyses of the mechanical behavior of soil and soil-rock mixture via the 3D direct shear test”, *Geomech. Eng.*, **9**(6), 815-827.
- Zhou, Z.L., Cai, X., Chen, L., Cao, W.Z., Zhao, Y. and Cheng, X. (2017), “Influence of cyclic wetting and drying on physical and dynamic compressive properties of sandstone”, *Eng. Geol.*, **220**, 1-12.
- Zhou, Z.L., Wu, Z.B., Li, X.B. and Xiang, L.I. (2015), “Mechanical behavior of sandstone under cyclic point loading”, *Trans. Nonferrous Met. Soc. Chin.*, **25**(8), 2708-2717.